

Tensions in the Optical Conductivity of Graphene

Marianne Moore^{1,2}

¹*Department of Physics and Astronomy, University of British Columbia, Vancouver, BC V6T 1Z1, Canada*

²*TRIUMF, 4004 Wesbrook Mall, Vancouver, BC V6T 2A3, Canada*

(Dated: December 19, 2020)

The theoretical predictions of the optical conductivity in graphene have been much debated in the past decade. When ignoring the Coulomb interaction, the electrons in graphene behave as free massless fermions. However, the Coulomb interaction is expected to be strong in graphene. Including this correction can be done through various techniques, but curiously, the resulting values of the conductivity do not always match. The results of these methods are discussed and compared. Strangely, none of the experiments that studied the optical conductivity found hints of electron-electron interaction effects, increasing the confusion surrounding this material property.

I. INTRODUCTION

Graphene is an atomically thin material made of carbon atoms arranged in a hexagonal lattice, represented in Figure 1. Even though it was discovered recently – in 2004 (see Ref. [1]) – many theoretical, numerical and experimental studies have been performed to better understand the properties of this two-dimensional material.

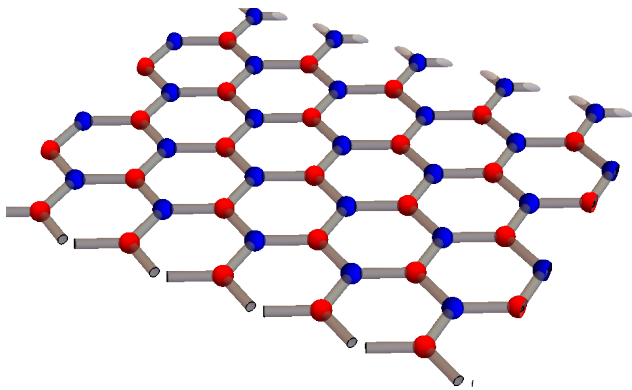


Figure 1. Representation of a single sheet of graphene. The red and blue balls represents the two carbon atoms of each unit cell.

One such interesting property is its optical conductivity. We can distinguish the AC and DC conductivities of a material by the type of voltage fed into the sample. However, electronic sources are not able to provide very large alternating currents. Instead, shining light perpendicularly on the sample naturally creates an alternating electric field in the plane of the two-dimensional material. This creates an experiment much simpler to perform than using a voltage source, and the name *optical* conductivity derives its name from the use of optical frequencies of light.

In general, the conductivity is a complicated function of the frequency ω , the momentum \mathbf{q} , the temperature T , the chemical potential μ , the scattering rate Γ and the gap Δ (when the system is an insulator). Due to this, most studies look in one of two limiting cases: the collisionfull ($\omega \ll \Gamma, T$) and collisionless ($\omega \gg \Gamma, T$) regimes

[2]. The first is relevant to the study of the DC limit ($\omega \rightarrow 0$), yet it can be hard to account for finite temperature and disorder. On the other hand, the collisionless limit is simpler to determine and comparable to experimental results obtained by shining visible light on the material. It assumes that electrons undergo many oscillations before experiencing a collision, such that the damping is vanishingly small. The many-body dynamics is dictated by the single particle trajectories. This is the limit we are going to explore in this paper. For simplicity, in the collisionless regime we set $\mu = \Delta = \mathbf{q} = \Gamma = T = 0$.

The conductivity is determined by the movement of electrons in the material, which in turns depends on the mass and velocity of these electrons. In the non-relativistic limit, the electronic dispersion relation is given by $E = k^2/(2m)$ and the electron mass can be determined by $(\partial^2 E/\partial k^2)^{-1}$. However, graphene is closer to the relativistic dispersion relation, $E = c|\mathbf{k}|$, in which the particle is the massless photon. Note that the energy is now linear, rather than quadratic, in the momentum. Using a tight-binding model for graphene with a , the shortest distance between two carbon atoms, and t , the nearest-neighbour hopping, the dispersion relation is $E = v_F|\mathbf{k}|$, where $v_F = 3ta/2$ is the Fermi velocity of electrons [3]. This is true near the touching points of the two bands, shown in Figure 2. In graphene, $v_F \approx c/300$, such that we find that for a sample at half filling, the conduction electrons are massless and propagate with velocity v_F . These electrons are called 2D Dirac fermions. It is important to remember that for higher energies, the approximation does not hold anymore, and the non-linearity of the band structure must be taken into account.

With this in mind, at first order we can approximate the optical conductivity of graphene by that of free fermions in two dimensions, giving $\sigma_0 = e^2/(4\hbar)$, independent of the probing frequency ω . This is the expression for clean graphene at half filling, and in the limit of zero temperature and no doping [4]. Clean graphene is free of disorder, impurities, inhomogeneities, rippling, etc [5].

However, electrons in graphene are not free and interact through the Coulomb potential. In vacuum, it is given

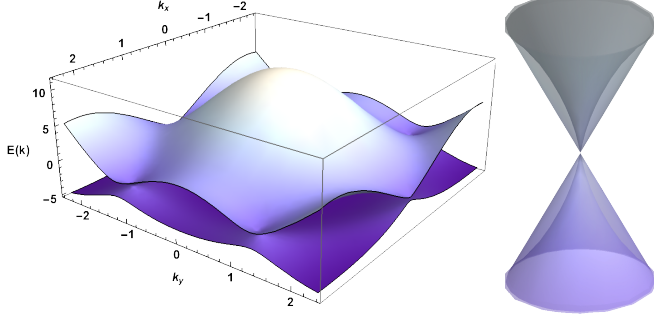


Figure 2. (left) Energy bands of graphene. (right) Zoom in at one of the touching points of the two bands. The cone represents the spectrum $E = \pm v_F |\mathbf{k}|$, while the curved cone illustrates the correction due to the renormalized Fermi velocity of electrons in graphene \tilde{v}_F . Inspired by [6].

by $V(r) = e^2/(4\pi\hbar cr) = \alpha_{\text{QED}}/r$, where α_{QED} is the fine structure constant of QED. In the case of graphene, the Coulomb potential becomes $V_g(r) = \alpha_g/r$, with its fine structure constant being $\alpha_g = e^2/(4\pi\hbar v_F) \approx 2.2^1$. Assuming the corrections due to the Coulomb force are weak compared to 1, we can express the conductivity as a perturbation expansion of σ_0 :

$$\sigma(\omega) = \sigma_0 (1 + \mathcal{C}_1 \alpha_g + \mathcal{O}(\alpha_g^2)). \quad (1)$$

The \mathcal{C}_i are interaction correction coefficients. Renormalization group for 2D Dirac fermions predicts that the Fermi velocity of graphene is a running constant, i.e. $v_F \rightarrow \tilde{v}_F(\omega)$ which depends on the frequency ω . Its effect is apparent in the shape of the energy bands of graphene near the touching points (see Fig. 2). The renormalized fine structure constant is then $\tilde{\alpha}_g(\omega)$ and given by

$$\tilde{\alpha}_g(\omega) = \frac{\alpha_g}{1 + \frac{1}{4}\alpha_g \ln(v_F \Lambda/\omega)}, \quad (2)$$

where Λ is the momentum cutoff [7].

Various methods have been developed to compute the conductivity and take into account the Coulomb interaction, namely the density-density response, the current-current response, the Boltzmann kinetic equation, tight-binding calculations, quantum Monte-Carlo simulations, and the Hartree-Fock approximation. All these approaches should yield the same result for each of the \mathcal{C}_i , but despite the apparent simplicity of the task, it is not the case.

¹ Physically, we should use $\alpha_g/\bar{\epsilon}$, where $\bar{\epsilon} = \frac{1}{2}(\epsilon_1 + \epsilon_2)$ is the average dielectric constant of the materials above and below the graphene sheet. This constant must be taken into account to compare the value of $\sigma(\omega)$ between experiments and theory.

The remainder of the paper is organized as follows: first, the linear response framework of the conductivity will be outlined in Section II. The free-fermion conductivity σ_0 will be discussed in Section III. Then techniques used to determine the corrections to the free-fermion conductivity for graphene will be elaborated in Section IV. Finally, the result of experiments will be mentioned in Section V.

II. LINEAR-RESPONSE THEORY

In electrodynamics, the current relates to the conductivity tensor and the electric field through

$$\langle \mathbf{j}(t) \rangle_{\mathbf{A}} = \int_{-\infty}^{\infty} dt' \overleftrightarrow{\sigma}(t-t') \mathbf{E}(t'), \quad (3)$$

using $\overleftrightarrow{\sigma}(t-t') = 0$ for $t-t' < 0$. This enforces that the response of the system is retarded: it can only be measured after the application of the drive. This also allows to define the Fourier transform of the convoluted functions. $\langle \mathbf{j}(t) \rangle_{\mathbf{A}}$ is the thermal average of the current operator $\mathbf{j}(t)$ evolved in the presence of a perturbing vector potential \mathbf{A} . In the presence of the perturbation, the total Hamiltonian reads $\mathcal{H} = \mathcal{H}_0 + \mathbf{j} \cdot \mathbf{A}$.

To devise an expression for the conductivity, we need to apply some interaction picture trick [8]. The current evolves in time as $\langle \mathbf{j}(t) \rangle_{\mathbf{A}} = \langle U_{\mathbf{A}}^{-1} \mathbf{j}(t) U_{\mathbf{A}} \rangle$, where

$$U_{\mathbf{A}}(t) = \mathcal{T} \exp \left(-i \int_{-\infty}^t dt' \mathbf{j}(t') \cdot \mathbf{A}(t') \right). \quad (4)$$

where \mathcal{T} indicates time ordering. Expanding the exponential perturbatively and neglecting the zeroth order term (there is no current without perturbation), one finds

$$\langle j^i(t) \rangle_{\mathbf{A}} = -i \int_{-\infty}^{\infty} dt' \theta(t-t') \underbrace{\langle [j^i(t), j^j(t')] \rangle}_{\overleftrightarrow{\Pi}^{ij}(t-t')} A^j(t') \quad (5)$$

$\overleftrightarrow{\Pi}^{ij}(t-t')$ is the retarded current-current polarization function. Finally, we want to connect Eqs. (3) and (5) to arrive at an expression for $\overleftrightarrow{\sigma}$. Making use of $\overleftrightarrow{\sigma} = -\nabla \rho - \partial_t \mathbf{A}$ for an electric field of the form $\mathbf{E} = \mathbf{E}_0 e^{-i\omega t}$, we find

$$\sigma^{ij} = \lim_{\mathbf{q} \rightarrow 0} \frac{\Pi^{ij}}{i\omega} = - \lim_{\mathbf{q} \rightarrow 0} \frac{i\omega}{|\mathbf{q}|^2} \Pi^{00}, \quad (6)$$

where in the second equality we used the continuity equation

$$\nabla \cdot \mathbf{j} = -\frac{\partial \rho}{\partial t}. \quad (7)$$

and Π^{00} is the density-density correlation function.

To understand why we take the limit $\mathbf{q} \rightarrow 0$, let's consider the relationship between frequency and momentum for light, $\omega = c|\mathbf{q}|$. To satisfy the condition of having a finite ω , we must take \mathbf{q} very small, i.e. to 0.

III. FREE-FERMION CONDUCTIVITY

The free-fermion conductivity can be represented as a one-loop diagram as shown in Figure 3, where the wiggly lines represent photons carrying momentum \mathbf{q} and frequency Ω and the straight lines represent fermions. Photon interact with two electrons through a vertex ($-ie\gamma^\mu$), here represented as a black dot.

The retarded polarization function can be related to the time-ordered response through analytic continuation. Condensing all components in a single expression and restoring the momentum dependence, we are interested in computing this object:

$$\Pi^{\mu\nu}(t, \mathbf{q}) = \langle \mathcal{T} j^\mu(t, \mathbf{q}) j^\nu(0, -\mathbf{q}) \rangle, \quad (8)$$

where $j^0 = \rho$, the charge density, \vec{j} is the charge current.

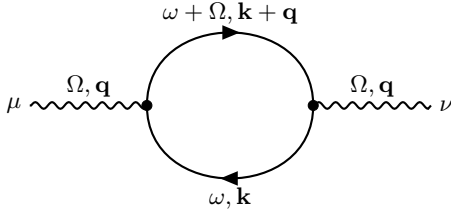


Figure 3. One-loop diagram with external frequency Ω and momentum q . The external photon lines represents the electric field in $\mathbf{j} = \sigma\mathbf{E}$.

Mathematically, the diagram reads

$$\Pi_1^{\mu\nu}(\Omega, \mathbf{q}) = i \text{Tr} \int_{\mathbf{k}} \int_{\omega} (-ie\gamma^\mu) G_{\omega+\Omega, \mathbf{k}+\mathbf{q}} (-ie\gamma^\nu) G_{\omega, \mathbf{k}} \quad (9)$$

where $G_{\omega, \mathbf{k}}$ is the Green's function for an electron carrying frequency ω and momentum \mathbf{k} . It is given by

$$G_{\omega, \mathbf{k}} = \frac{i\mathbf{k}}{k^2} = i \frac{\gamma^0 \omega - v_F \boldsymbol{\gamma} \cdot \mathbf{k}}{\omega^2 + v_F^2 \mathbf{k}^2}. \quad (10)$$

Here we integrate over all possible four-momenta (ω, \mathbf{k}) that can be carried by the electron-positron pair, using the abbreviation $\int_{\mathbf{k}} \int_{\omega} = \int \frac{d^2 \mathbf{k}}{(2\pi)^2} \int \frac{d\omega}{2\pi}$. The momentum space integral is two-dimensional since we consider the conductivity for graphene, a two-dimensional material.

Performing the integrals requires to perform the trace, introduce a renormalization scale μ , go to Euclidian space ($\omega = i\omega_E$), and use the standard rules for integrating Feynman diagrams.

As a final comment, the current-current correlation function that we would consider is not that of isolated components Π_1^{11} and Π_1^{22} , but rather

$$\sigma(\omega) = \lim_{\mathbf{q} \rightarrow 0} \frac{1}{i\omega} \frac{\Pi_1^{11}(\omega, \mathbf{q}) + \Pi_1^{22}(\omega, \mathbf{q})}{2}. \quad (11)$$

The reason behind this comes from symmetry considerations. We can express the optical conductivity as a 2×2 matrix as

$$\sigma_{ij} = \begin{pmatrix} \sigma_{xx} & \sigma_{xy} \\ \sigma_{yx} & \sigma_{yy} \end{pmatrix} \quad (12)$$

$$= \frac{\sigma_{xx} + \sigma_{yy}}{2} \mathbb{1} + \frac{\sigma_{xx} - \sigma_{yy}}{2} \sigma_z \quad (13)$$

From line (12) to (13), the off-diagonal elements are removed because there is no magnetic field, so we are not expecting a response in any direction where we do not have an electric field. Using rotational symmetry, we can get rid of the σ_z term, leaving us with $\sigma_{ij} = (\sigma_{xx} + \sigma_{yy})/2$. This is the term that gives rise to $(\Pi_1^{11} + \Pi_1^{22})/2$ in Equation (11).

The density-density (Π^{00}) and current-current ($\Pi^{11} + \Pi^{22}$) techniques mentioned above are the diagrammatic ways that can be used to obtain the free-fermion conductivity.

Many other methods exist to compute the free-fermion conductivity, but as they all yield the same result, they will not be covered here. However, where they differ is when we introduce interactions.

IV. ELECTRON-ELECTRON INTERACTIONS IN GRAPHENE

It is worth wondering if the electron interactions either dominate the physics or are irrelevant. In Equation (1), we expressed the conductivity as a perturbative expansion of the non-interacting conductivity σ_0 . For a perturbative series to be convergent, we expect \mathcal{C}_1 to be very small, especially since $\alpha_g \approx 2.2$.

To investigate the strength of electron interactions, let's focus on long-range Coulomb interaction; it was shown that there is no short-range (or on-site) interaction [2]. Graphene has a null Fermi surface at the touching points of the two bands and its Fermi momentum k_F is 0. Due to this, its Thomas-Fermi wavelength λ_{TF} diverges while its Thomas-Fermi momentum k_{TF} goes to 0. Consequently, Coulomb interactions in graphene are unscreened, and given by

$$V_{\mathbf{k}} = \frac{4\pi\alpha_g}{|\mathbf{k}|}. \quad (14)$$

In order to get screening, one would need to dope the system with electrons and get away from the vanishing Fermi surface. Furthermore, the electron-electron interactions are considered instantaneous because the electron velocity is much smaller than that of the photons – which mediate the Coulomb interaction – such that retarded effects are negligible [3]. From Equation (14), we can define the Coulomb energy per electron to be $E_C \approx e^2 n_e^{1/2}$, where $n_e = 1/l^2$ is the average electron density in 2 spatial dimensions.

On the other hand, as mentioned in the introduction, the kinetic energy in graphene is $E = v_F |\mathbf{k}|$, which gives $E_K \approx v_F n_e^{1/2}$ per electron. Then the ratio of Coulomb to kinetic energy is $E_C/E_K \propto e^2/v_F$, independent of the electronic density [5]. Thus, the strength of the Coulomb interaction relative to the kinetic energy is determined by the material properties; it is in fact non-trivial and important in the study of material properties such as the optical conductivity.

In order to account for first-order electron interactions, the current-current and density-density methods require to sum all two-loop diagrams; these are the terms we need in order to determine the coefficient \mathcal{C}_1 . There exists three such diagrams, the vertex correction (Figure 4) and two self-energy corrections (Figure 5) – the factor of two coming from the fact that the extra photon can couple either to the $\mathbf{k} + \mathbf{q}$ or to the \mathbf{k} fermion. As we will be taking \mathbf{q} , the external momentum, to 0, both terms will

give the same contribution and we only need to solve one self-energy diagram and multiply the answer by two. Converting the diagrams into equations, this gives the two expressions:

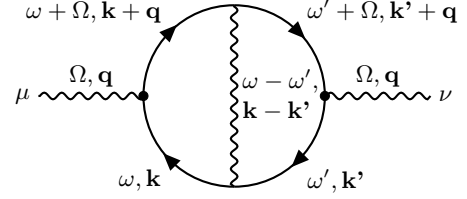


Figure 4. Two-loop vertex correction diagram with external frequency Ω and momentum q .

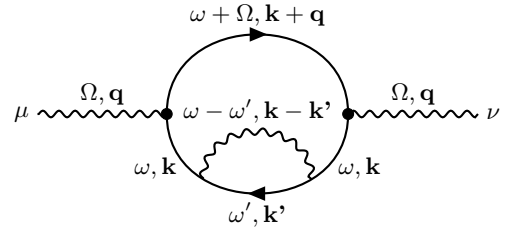


Figure 5. Two-loops self-energy correction diagram with external frequency Ω and momentum q . There are two such diagrams, as the photon can couple either to the electron or to the positron (top or bottom branch).

$$\Pi_{2, \text{vertex}}^{\mu\nu}(\Omega, \mathbf{q}) = i \text{Tr} \int_{\mathbf{k}, \mathbf{k}'} \int_{\omega, \omega'} V_{\mathbf{k}-\mathbf{k}'} G_{\omega', \mathbf{k}'} G_{\omega, \mathbf{k}} (-ie\gamma^\mu) G_{\omega+\Omega, \mathbf{k}+\mathbf{q}} G_{\omega'+\Omega, \mathbf{k}'+\mathbf{q}} (-ie\gamma^\nu) \quad (15)$$

and

$$\Pi_{2, \text{self}}^{\mu\nu}(\Omega, \mathbf{q}) = i \text{Tr} \int_{\mathbf{k}, \mathbf{k}'} \int_{\omega, \omega'} V_{\mathbf{k}-\mathbf{k}'} G_{\omega, \mathbf{k}} G_{\omega', \mathbf{k}'} G_{\omega, \mathbf{k}} (-ie\gamma^\mu) G_{\omega+\Omega, \mathbf{k}+\mathbf{q}} (-ie\gamma^\nu) \quad (16)$$

When computing these loops using either the current-current ($\mu = \nu = \{1, 2\}$) or density-density ($\mu = \nu = 0$) method, the integrals diverge logarithmically in the UV. However, the sum $\Pi_{2, \text{vertex}}^{\mu\nu} + 2\Pi_{2, \text{self}}^{\mu\nu}$ is finite, but varies depending on the approach taken to evaluate the diagrams. Values that appear in the literature (see e.g. Refs. [9] and [10]) for \mathcal{C}_1 are

$$\begin{cases} \mathcal{C}_1^1 = \frac{19-6\pi}{12} \approx 0.013 \\ \mathcal{C}_1^2 = \frac{11-3\pi}{6} \approx 0.263 \\ \mathcal{C}_1^3 = \frac{25-6\pi}{12} \approx 0.512 \end{cases} \quad (17)$$

The various methods to regularize the divergent integrals are the usual quantum field theory techniques and include subtracting the $\omega = 0$ contribution, dimensional

regularization, Wilson momentum shell renormalization group, and modified minimal subtraction ($\overline{\text{MS}}$). The issues that give rise to the discrepancy (17) are (i) correctly implementing the technique used for all the theory, and not just a part of it (e.g. subtracting all the counterterms consistently, order by order [11]), (ii) ensuring charge conservation through the Ward identity, and (iii) the order in which we take the dimension d to 2 (i.e. take $\epsilon \rightarrow 0$) and the momentum cutoff Λ to infinity² [7].

² In dimensional regularization, diagrams are computed as analytic functions of the dimensionality of spacetime d . The final expression is then obtained by setting $d \rightarrow 2$, the physical dimension of the system. In reality, setting $d = 2$ causes problems; the way

Correctly regularizing the divergent integrals yield the value \mathcal{C}_1^1 for both current-current and density-density response. This value has been corroborated by the Boltzmann kinetic equation in the presence of an electric field

$$\frac{\partial f_{\mathbf{p}}}{\partial t} + ivp[\sigma_{\mathbf{p}}, f_{\mathbf{p}}] + e\mathbf{E} \cdot \frac{\partial f_{\mathbf{p}}}{\partial \mathbf{p}} = i \sum_{\mathbf{p}'} V_{\mathbf{p}-\mathbf{p}'} [f_{\mathbf{p}'}, f_{\mathbf{p}}] \quad (18)$$

and using a soft momentum cutoff (small momentum, to be distinguished from a hard cutoff, normally in the UV)[9]. $f_{\mathbf{p}}$ is the 2×2 matrix distribution function, where the right-hand side accounts for the lowest order electron-electron interaction.

Another technique that has been used is quantum Monte-Carlo simulations, performed by Boyda *et al* [12]. The benefit of this method is that it allows to account for interactions in a non-perturbative way. They found $\mathcal{C} \approx 0.01$, a similar value to \mathcal{C}_1^1 .

Two tight-binding computations have been completed, one by Link *et al.* [7] and one by Rosenstein *et al.* [13]. While the first group gets \mathcal{C}_1^1 , the second finds \mathcal{C}_1^2 . However, Link *et al.* carefully analyzed the results from the other group; they noticed that the authors regularized their divergent integrals in a way that violates charge conservation, and confused the Brillouin zone restricted with the unrestricted momentum integration. Thus, tight-binding results seem to agree with the value of \mathcal{C}_1^1 .

However, Stauber *et al.* [14] recently used a self-consistent Hartree-Fock approach and found $\mathcal{C} = 1/4$, a value which is more consistent with \mathcal{C}_1^2 , adding to the confusion surrounding the effect of electron-electron interactions in graphene.

V. EXPERIMENTAL DATA

Experimentally, the optical conductivity is determined by shining light onto a sample of graphene and determining the absorbance of the monolayer material. So far, three groups have attempted the measurement, and interestingly, they all published their results the same year: 2008.

The main conclusion from the three groups is that electron interactions are irrelevant, up to the sensitivity they achieved experimentally. A sketch of the values they obtained is presented in Figure 6.

Zhiqiang Li *et al.* [15] investigated the infrared spectral range of the optical conductivity, with photon frequency of $\omega \in [0.01, 0.16]$ eV, cooled down at a temperature of 45 K (0.004 eV). Their graphene samples were on

a SiO₂/Si substrate. They determined that their scattering rate was $\Gamma(\omega) \approx 0.0006$ eV, with $\Gamma(\omega)$ increasing with ω due to electron-electron and electron-phonon interactions, yet remaining much lower than ω . We notice that here the collisionless regime is approximately respected, as $\omega \gg T, \Gamma$. They found the optical conductivity to be $\sigma = (1.00 \pm 0.15)\sigma_0$ for $\omega \in [0.08, 0.13]$ eV, and stated that they could not determine without a doubt the conductivity outside of this range due to increasing uncertainties.

On the other hand, Kin Fai Mak *et al.* [16] measured the optical conductivity in the visible spectral range, with $\omega \in [0.2, 1.2]$ eV at room temperature (0.025 eV). Their graphene samples were deposited on a SiO₂ substrate. They found $\sigma = (1.0 \pm 0.1)\sigma_0$ for $\omega \in [0.5, 1.2]$ eV. For lower values of frequencies, they identified a deviation from σ_0 that they could account for by correcting for the non-zero chemical potential μ due to spontaneous doping of the graphene samples, as well as the finite temperature. Adding this correction term, they determined μ to be 100 meV and 200 meV for the two samples they studied. At low photon frequencies, T/ω is no longer negligible.

Finally, Rahul Raveendran Nair *et al.* [17] explored the optical conductivity in the optical range $\omega \in [1, 5]$ eV, probably at room temperature, though this is not stated in their paper nor in their supplemented material. They deposited their samples on a SiO₂ substrate. They observed $\sigma = (1.01 \pm 0.04)\sigma_0$ for $\omega \in [1, 2.5]$ eV. Above 2.5 eV, they find deviations from σ_0 , which they assume account for surface contamination by hydrocarbons, and possibly a long-range tail of the plasmon resonance located at 5 eV.

This team also studied multi-layered graphene and found that the opacity is proportional to the number N of layers involved; they observed $A \approx N\pi\alpha$, where α is the fine structure constant in vacuum. They determined that this rule holds at least for $N \leq 4$, but further theoretical analysis is required to better understand multi-layered graphene.

Overall, the three teams determined the optical conductivity of graphene to be consistent with the free fermion model conductivity σ_0 , without any noticeable contribution from electron interactions. The experimentalists do not attribute the deviations they find to interactions. It is important to note that the experiments do not directly probe the optical conductivity, i.e. the conductivity at zero momentum, and with a frequency in the visible range of the spectrum. Rather, they investigate the optical properties of graphene: its absorbance A , transmittance T , and reflectance R . The optical conductivity is determined by $\sigma = Ac/4\pi$. The transmittance is given by $T = (1 + A/2)^{-2}$ while the reflectance is $R = 1/4A^2T$.

A better analysis of the various parameters affecting the conductivity would be required to determine whether the electron interactions really play a role, such as the temperature, chemical potential, substrate, scattering rate, etc [2].

around it is to expand around $d = 2 - \epsilon$ by taking ϵ to 0.

$$\lim_{\epsilon \rightarrow 0} \left[\lim_{\Lambda \rightarrow \infty} \mathcal{C}(\epsilon, \frac{\omega}{\Lambda}) \right] = \mathcal{C}_2 \quad \lim_{\Lambda \rightarrow \infty} \left[\lim_{\epsilon \rightarrow 0} \mathcal{C}(\epsilon, \frac{\omega}{\Lambda}) \right] = \mathcal{C}_1$$

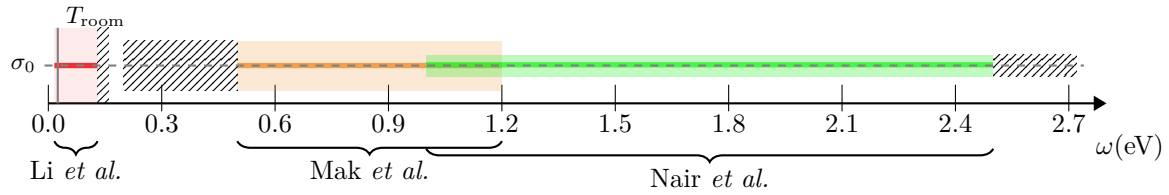


Figure 6. Experimental results of the optical conductivity obtained by three experimental groups. Shaded regions correspond to the quoted uncertainty in the measurements, and dashed regions represent where measurements have been performed but were inconclusive (see text for explanations of these null results). For comparison, the room temperature (0.025 eV) is shown.

VI. DISCUSSION

The optical conductivity of graphene has been the subject of debates in the past decade. Many condensed matter physicists have attempted understanding the effect of Coulomb interaction on the electrons of the material, getting various results. Although \mathcal{C}_1^1 is the value for which most theoretical studies agree, one cannot rigorously con-

clude that it is the correct result. On the experimental side, strangely, no interaction effect is detected, which is also very puzzling. More detailed analyses are required to fully comprehend the optical conductivity of graphene.

ACKNOWLEDGMENTS

The author would like to thank Vladimir Juričić and Pedro L. S. Lopes for useful discussions.

-
- [1] K. S. Novoselov, A. K. Geim, S. V. Morozov, D. Jiang, Y. Zhang, S. V. Dubonos, I. V. Grigorieva, and A. A. Firsov, *Electric field effect in atomically thin carbon films*, Science **306**, 666 (2004).
- [2] S. Teber, *Field theoretic study of electron-electron interaction effects in Dirac liquids*, habilitation thesis, e-print: <https://arxiv.org/abs/1810.08428> (2017).
- [3] A. H. Castro Neto, F. Guinea, N. M. R. Peres, K. S. Novoselov, and A. K. Geim, *The electronic properties of graphene*, Rev. Mod. Phys. **81**, 109 (2009).
- [4] T. Stauber, N. M. R. Peres, and A. K. Geim, *Optical conductivity of graphene in the visible region of the spectrum*, Phys. Rev. B **78**, 085432 (2008).
- [5] V. N. Kotov, B. Uchoa, V. M. Pereira, F. Guinea, and A. H. Castro Neto, *Electron-Electron Interactions in Graphene: Current Status and Perspectives*, Rev. Mod. Phys. **84**, 1067 (2012).
- [6] D. C. Elias, R. V. Gorbachev, A. S. Mayorov, S. V. Morozov, A. A. Zhukov, P. Blake, L. A. Ponomarenko, I. V. Grigorieva, K. S. Novoselov, F. Guinea and A. K. Geim, *Dirac cones reshaped by interaction effects in suspended graphene*, Nature Phys. **7**, 701 (2011).
- [7] J. M. Link, P. P. Orth, D. E. Sheehy, and Jörg Schmalian, *Universal collisionless transport of graphene*, Phys. Rev. B **93**, 235447 (2016).
- [8] A. Atland and B. D. Simons, *Condensed Matter Field Theory*, 2nd edition, Cambridge University Press, 770 p. (2010).
- [9] E. G. Mishchenko, *Minimal conductivity in graphene: Interaction corrections and ultraviolet anomaly*, EPL **83**, 17005 (2008).
- [10] V. Juričić, O. Vafek, and I. F. Herbut, *Conductivity of interacting massless Dirac particles in graphene: Collisionless regime*, Phys. Rev. B **82**, 235402 (2010).
- [11] D. Muñoz-Segovia and A. Cortijo, *Many-body effects in nodal-line semimetals: Correction to the optical conductivity*, Phys. Rev. B **101**, 205102 (2020).
- [12] D. L. Boyda, V. V. Braguta, M. I. Katsnelson, and M. V. Ulybyshev, *Many-body effects on graphene conductivity: Quantum Monte Carlo calculations*, Phys. Rev. B **94**, 085421 (2016).
- [13] B. Rosenstein, M. Lewkowicz, and T. Maniv, *Chiral Anomaly and Strength of the Electron-Electron Interaction in Graphene*, Phys. Rev. Lett. **110**, 066602 (2013).
- [14] T. Stauber, P. Parida, M. Trushin, M. V. Ulybyshev, D. L. Boyda, and J. Schliemann, *Interacting Electrons in Graphene: Fermi Velocity Renormalization and Optical Response*, Phys. Rev. Lett. **118**, 266801 (2017).
- [15] Z. Q. Li, E. A. Henriksen, Z. Jiang, Z. Hao, M. C. Martin, P. Kim, H. L. Stormer, and D. N. Basov, *Dirac charge dynamics in graphene by infrared spectroscopy*, Nature Phys. **4**, 532 (2008).
- [16] K. F. Mak, M. Y. Sfeir, Y. Wu, C. H. Lui, J. A. Misewich, and T. F. Heinz, *Measurement of the Optical Conductivity of Graphene*, Phys. Rev. Lett. **101**, 196405 (2008).
- [17] R. R. Nair, P. Blake, A. N. Grigorenko, K. S. Novoselov, T. J. Booth, T. Stauber, N. M. R. Peres, and A. K. Geim, *Fine Structure Constant Defines Visual Transparency of Graphene*, Science **320**, 1308 (2008).